

Nov 10th, 12:00 AM - 12:00 AM

## Experimental Investigation of the Effect of Screw Fastener Spacing on the Local and Distortional Buckling Behavior of Built-Up Cold-Formed Steel Columns

David C. Fratamico

Shahabeddin Torabian

Kim J. R. Rasmussen

Benjamin W. Schafer

Follow this and additional works at: <https://scholarsmine.mst.edu/isccss>



Part of the [Structural Engineering Commons](#)

---

### Recommended Citation

Fratamico, David C.; Torabian, Shahabeddin; Rasmussen, Kim J. R.; and Schafer, Benjamin W., "Experimental Investigation of the Effect of Screw Fastener Spacing on the Local and Distortional Buckling Behavior of Built-Up Cold-Formed Steel Columns" (2016). *International Specialty Conference on Cold-Formed Steel Structures*. 1.

<https://scholarsmine.mst.edu/isccss/23iccfss/session8/1>

This Article - Conference proceedings is brought to you for free and open access by Scholars' Mine. It has been accepted for inclusion in International Specialty Conference on Cold-Formed Steel Structures by an authorized administrator of Scholars' Mine. This work is protected by U. S. Copyright Law. Unauthorized use including reproduction for redistribution requires the permission of the copyright holder. For more information, please contact [scholarsmine@mst.edu](mailto:scholarsmine@mst.edu).

## **Experimental Investigation of the Effect of Screw Fastener Spacing on the Local and Distortional Buckling Behavior of Built-Up Cold-Formed Steel Columns**

David C. Fratamico<sup>1</sup>, Shahabeddin Torabian<sup>2</sup>,  
Kim J. R. Rasmussen<sup>3</sup>, Benjamin W. Schafer<sup>4</sup>

### **Abstract**

This paper addresses an ongoing experimental and computational effort on the buckling and strength of built-up cold-formed steel (CFS) columns. Specifically, two 6 in. (152 mm) deep lipped channel sections (i.e. the 600S137-54 and 600S162-54 using AISI S200-12 nomenclature) are studied here in a back-to-back, screw-connected form and were chosen for their local and distortional slenderness to study the effect of fastener spacing and layout on local and distortional buckling and collapse behavior. Thirty column tests are completed with concentric loading. The screw spacing is varied from  $L$  to  $L/6$ , where  $L$  is the column length, with and without varying lengths of End Fastener Groups (EFG), which are a prescriptive layout of fasteners at the ends of built-up columns that is required by AISI S100-12 and is intended to insure end rigidity and increase composite action. Results yield two general types of deformation modes: compatible (where the connected webs conform to the same buckling shape) and isolated stud buckling. Buckling loads and half-wavelengths of deformation are shown to be affected by the tighter screw spacings. EFGs increase compatibility of buckling, but prove to be an inefficient (costly) method of fastening studs together. Future work includes expanding the design methods for built-up CFS columns to explicitly account for local and distortional buckling behavior of the built-up section, and to develop efficient numerical tools supporting a new design method under development.

---

<sup>1</sup> Ph.D. Student, Johns Hopkins University, Baltimore, MD <fratamico@jhu.edu>

<sup>2</sup> Assistant Research Professor, Johns Hopkins University, Baltimore, MD  
<torabian@jhu.edu>

<sup>3</sup> Professor, University of Sydney, Sydney, NSW, Australia  
<kim.rasmussen@sydney.edu.au>

<sup>4</sup> Professor, Johns Hopkins University, Baltimore, MD, <schafer@jhu.edu>

## 1. Introduction

Framed Cold-Formed Steel (CFS) structures are composed of lightweight, often panelized systems that can be locally strengthened with the use of built-up sections. If greater local system rigidity is required or high axial or bending loads are expected, built-up members (composed in a typical welded, screw-fastened, or bolted traditional, doubly-symmetric back-to-back “I” or toe-to-toe “box” sections) can be easily installed in framing and designed as shear wall chord studs, headers, jambs, truss-members, or even unsheathed stand-alone columns. Built-up CFS columns made with two lipped-channel studs, for example, can deliver an axial compression capacity of more than twice that of the individual members through composite action, which is enabled through the fasteners. The degree of connectivity between connected studs and its effect on buckling and post-buckling capacities is a primary motivation for the research presented herein.

The current North American cold-formed steel specification (AISI-S100 2012) contains limited guidelines on the design of built-up CFS columns, but research has partly addressed this issue. Stone and LaBoube (2005) conducted a set of column experiments with back-to-back CFS channel sections and found that the AISI-S100 (2012) modified slenderness ratio can be conservative and that while the bearing end conditions are important for maintaining column strength the code prescribed End Fastener Groups (EFG) may not be necessary for framed members. Further experiments were conducted on built-up CFS sections with intermediate stiffeners by Young and Chen (2008); they concluded that using only the single section properties in the Direct Strength Method (DSM) for calculating nominal local and distortional capacities of built-up sections provided acceptable, but conservative estimates of the strength. Other experimental work on various types of built-up CFS column cross-sections using combinations of Zee, track, and sigma sections compared tested strengths with results from DSM-based equations that were calibrated to account for buckling interactions (Georgieva et al. 2012). Similar testing of varying cross-sections and DSM calibration was completed and an efficient approach to model web interconnections using scaling factors for the web thickness were explored at the University of Hong Kong (Zhang 2014). Built-up beams of varying cross-sections, screw arrangements, web perforations, and intermediate stiffeners were also tested at the University of Hong Kong; numerical models were completed and DSM design approaches were proposed (Wang 2015). Experiments on local and flexural buckling of battened built-up CFS columns were completed by Anbarasu et al. (2015) and Dabao et al. (2015); the former assessed the conservatism of two DSM design approaches and the latter concluded that strengths from AISI S100 (2007) are non-conservative for columns failing in local buckling and conservative for those failing in flexural buckling.

Current design codes may inadequately predict the effect of fastener spacing on built-up CFS column capacity when multiple deformation modes exist, specifically modes other than flexural buckling. The 2005 AS/NZS 4600 Standard limits only the maximum fastener spacing along the column length by checking that flexural buckling of the individual uprights between fasteners will not occur prior to global flexural buckling of the built-up section. In the U.S., AISI-S100 (2012) Section D1.2 requires the calculation of the axial capacity of built-up columns using the modified slenderness ratio approach, as adopted from AISC 360 (2010) which assumes only flexural buckling in the estimation of strength. It cannot predict the effects of fastener spacing, layouts, and stiffness on the torsional, flexural-torsional, distortional, or local buckling modes that frequently drive failure in sheathed columns (Fratamico et al. 2016). Built-up members subject to pure flexural buckling are only prescribed a limiting maximum fastener spacing of the lesser of either  $L/6$  or a factor dependent on the tensile strength of a single connection. AISI-S100-12 also requires the use of a special End Fastener Group (EFG) at the member ends, as a prescriptive design measure when screws are selected instead bolts or welds. Thus, its impact on the modified slenderness is not treated directly. Section D1.2 specifies that screws in the EFG must be longitudinally spaced at 4 diameters apart or less and for a distance equal to 1.5 times the maximum width of the member. These groups are superimposed on the layout of evenly-spaced fasteners required by code.

The work presented herein follows numerical studies by the first author in which the level of composite action was varied in built-up CFS columns employing finite element (FE) and finite strip (FS) models undergoing elastic buckling. Nodal multi-point constraints and discrete elastic nodal springs were used to model fasteners in the FE model, and smeared longitudinal constraints were used in the FS model. Example results included an 85% increase in composite action with the addition of both smeared and discrete fasteners (Fratamico and Schafer 2014). Fratamico et al. (2015) also numerically studied the effects of adding EFGs to models and using a parametric layout of spacings and stiffnesses in an FE model to explore partially composite action. Recently, a series of 16 tests were also performed in which screw-fastened, back-to-back, sheathed and unsheathed built-up CFS columns were tested to understand prevailing deformation modes beyond flexural buckling (Fratamico et al. 2016). This paper presents tests for understanding the effect of web fastener layouts and spacing on the local and distortional buckling and collapse behavior of back-to-back CFS columns. Experimental tests are performed in lieu of numerical modeling at this stage, since efficient modeling methods of screw fasteners are currently in progress. Also sought are the fastener spacings which can affect formation of local buckling half-waves in the webs, as well as the degree of compatible deformations (and potential higher stiffness or capacities, as a result) among the two studs.

## 2. Built-Up Cold-Formed Steel Column Testing

### 2.1 Testing Overview

In this paper, 30 built-up CFS column tests are detailed and their results are reported. Two 6 in. (152 mm) deep lipped channel sections are used: the 600S162-54 and 600S137-54 sections (using AISI-S200-12 nomenclature). The 600S137-54 section (previously used in beam-column tests in our lab (Torabian et al. (2015))) nominally has a 6 in. (152 mm) web, 1.375 in. (34.9 mm) flange, 0.375 in. (9.5 mm) lip, and a thickness of 0.0566 in. (1.43 mm). These sections were chosen for their local and distortional slenderness and are both common in design. The selected column height, to potentially allow local and/or distortional buckling is 3 ft (0.91 m), providing enough length for at least one distortional buckling half wavelength of 14.5 in. (36.8 cm) to develop without significant impact from the end boundary conditions. The reported buckling half-wavelength is obtained from a signature curve analysis of a single section using CUFSM (Schafer and Adány 2006). Local buckling is also expected from the various fastener layouts used in the tests, with a half-wavelength of 4.5 in. (11.4 cm).

The column studied is composed of a back-to-back “I” section as shown in Fig. 1, with #10 sized self-drilling hex washer head screws connecting the webs of two equivalently-sized channel sections, of both section types mentioned earlier. Fastener layouts are designed and installed according to AISI S100-12 (2012) sections D1.2 and E4.2, including the end fastener groups (EFG). The parametric fastener layouts are described in the following sections.

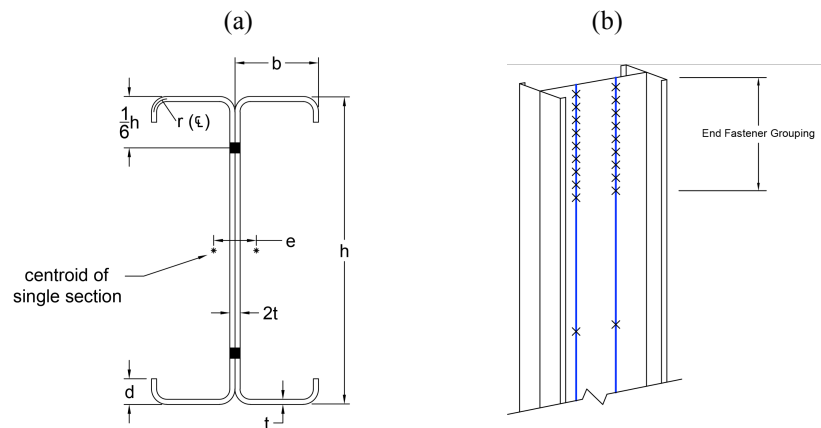


Figure 1. (a) The built-up, back-to-back section studied, showing the location of web screws and (b) an example of the fastener group layout at the column ends



Testing requires monotonic, concentric compression loading using a 100 kip (445 kN) MTS universal testing rig with fixed platens that bear directly on tracks, which are installed on either end of the columns. Figure 2 shows the MTS rig setup. The tests were displacement-controlled with a load rate not exceeding 0.015 in/min (0.38 mm/min). All other components of the test setup are described and shown in the following section.

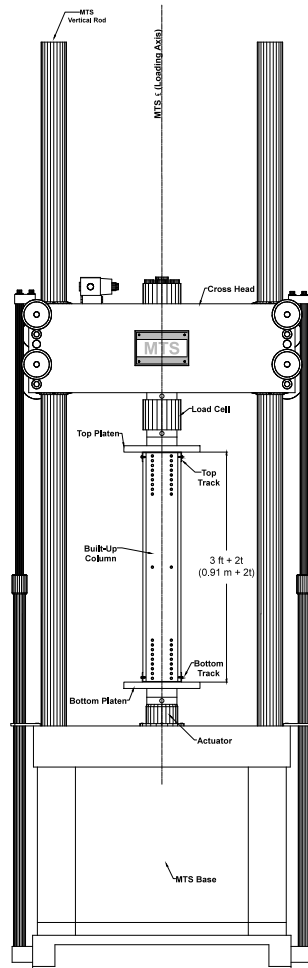


Figure 2. MTS rig setup (elevation)

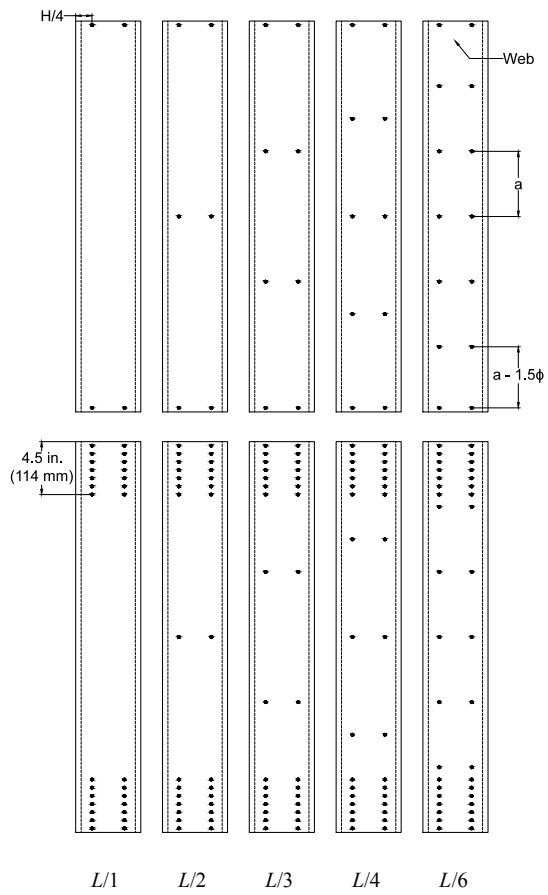


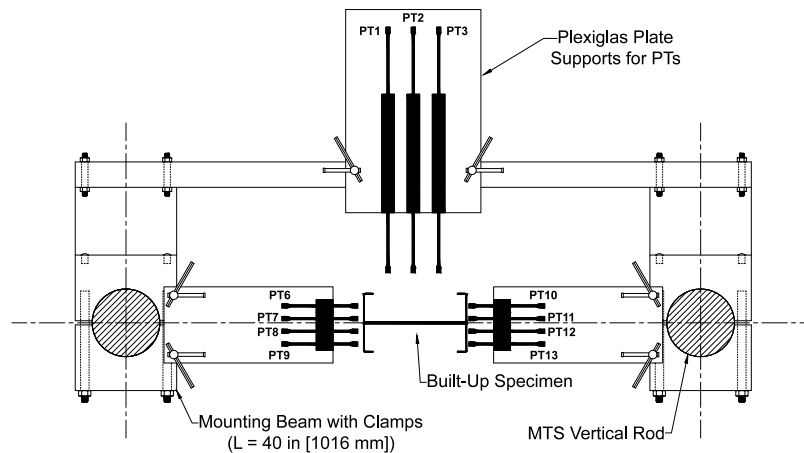
Figure 3. Parametric fastener layout on column webs; examples for A-series (top) and C-series (bottom)

**Table 2. Position of evenly-spaced fasteners for all spacings**

Trial (B-series as example)	Layout	Spacing, $a$ [in.] (cm)*
B1	$L/1$	36 (91)
B2	$L/2$	18 (46)
B3	$L/3$	12 (31)
B4	$L/4$	9 (23)
B5	$L/6$	6 (15)

\*Note: an offset of 1.5 times the nominal screw diameter  $\phi$  of 0.375 in. (9.5 mm) from the ends of the column must be applied to the top and bottom fastener pairs

A calibrated load cell on the MTS rig (Fig. 2) measures force, and the MTS rig's LVDT measures the applied axial displacements. To track specimen deformations, 15 position transducers (PTs) are installed. Lateral bi-planar displacements, overall rotation, and distortion of the cross-section at mid-height can be tracked throughout the test using 11 PTs as shown in Fig. 4. In addition, 1 PT is installed on the top and bottom tracks, orthogonal to the web of the studs in order to measure local buckling or localized failures at the stud web plate ends that are in contact with the tracks. To monitor stud engagement to the track during the tests a PT is installed at the top and at the bottom track. LabVIEW software and National Instruments hardware are used for data acquisition. The error of eccentricity and out-of-plumbness are recorded for each specimen as they are loaded into the rig. Measurements were taken in two planar directions at the top, middle, and bottom of the specimens to ensure that the centroids coincided with the line of action of the applied load. Error values are recorded at the final position, and are always less than 0.025 in. (0.64 mm). Note, no PTs were attached to specimens A1b and A1c in order to accommodate a portion of the joint work with Lama Salomon, et al. (2016) on 4D image-based reconstruction.

**Figure 4. MTS test rig setup (top-down view at mid-height)**

### 2.3 Geometric Imperfections and Material Characterization

Measurements for specimen dimensions and quantification of geometric imperfections were completed using a novel laser scanning method at Johns Hopkins University (Zhao et al. 2015). Full-field 3D geometric information is obtained as a point cloud of stitched longitudinal scan readings from multiple scan angles. Average plate thickness for each specimen was measured by hand using a calibrated micrometer, and the results can be used in finite strip analyses and in the reconstruction of the 3D geometry for each specimen. Final results are not reported here since the scan data is currently being post-processed; however, sample output data is shown in Fig. 5, and results are discussed in Zhao and Schafer (2016) and in the first author's forthcoming thesis.

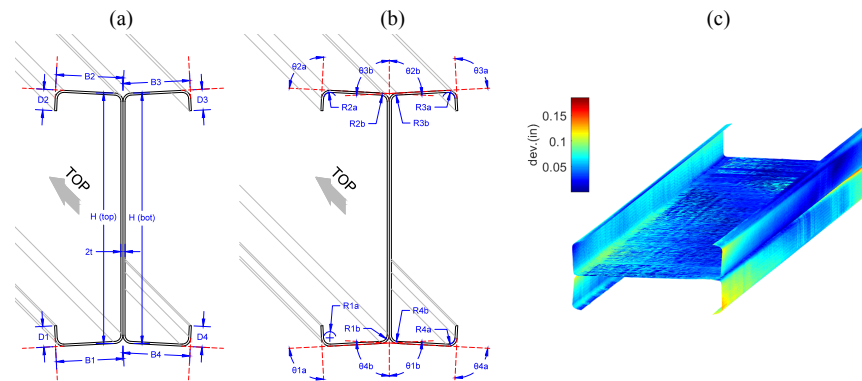


**Figure 5. Imperfection results from scans: (a) cross-section dimensions averaged over full length, (b) averaged cross-section angles and radii, and (c) full-field 3D reconstruction**

To quantify the basic material properties of the CFS studs and tracks used for the test specimens, a series of 10 coupon tests were completed using CNC milled longitudinal cuts of the webs (W1 & W2) and flanges (F1 & F2) for the channel sections and of the webs (W) and lips (L) of the track section, in accordance with ASTM A370-12a (2012). Table 3 shows the results. The average yield stress for the 600S137-54 and 600S162-54 sections are 57.3 ksi (394 MPa) and 57.4 ksi (396 MPa), respectively; the nominal yield stress is 50 ksi (345 MPa). Young's modulus was not estimated from the linear data in the test results, but rather taken as 29,500 ksi (203 GPa) as prescribed in AISI S100-12.

**Table 3. Tensile coupon test results**

Specimen	Base Metal Thickness t [in.] (mm)	Gauge Elongation $\Delta L_g$ [%] <sup>1</sup>	Yield Strength $F_{y,0.2}$ [ksi] (MPa) <sup>2</sup>	Tensile Strength $F_u$ [ksi] (MPa)	Strain at Tensile Strength $\epsilon_u$ [%]
600S137-W1	0.055 (1.39)	21.6	58.3 (402)	70.3 (485)	15.4
600S137-W2	0.055 (1.39)	23.5	57.7 (398)	69.8 (481)	17.7
600S137-F1	0.055 (1.39)	23.3	56.5 (389)	69.9 (482)	18.0
600S137-F2	0.054 (1.37)	23.7	56.5 (389)	69.7 (481)	17.8
Mean	0.055 (1.39)		57.3 (394)	69.9 (482)	
C.o.V.	0.006		0.016	0.006	
600S162-W1	0.055 (1.40)	24.4	57.8 (398)	69.7 (480)	17.8
600S162-W2	0.055 (1.39)	22.2	57.9 (399)	69.7 (481)	17.6
600S162-F1	0.054 (1.38)	21.7	57.2 (395)	69.5 (479)	16.4
600S162-F2	0.054 (1.38)	23.0	56.7 (391)	70.1 (483)	18.0
Mean	0.055 (1.39)		57.4 (396)	69.8 (481)	
C.o.V.	0.008		0.010	0.004	
600T150-W	0.055 (1.39)	22.0	59.6 (411)	71.3 (492)	17.1
600T150-L	0.055 (1.39)	23.6	58.8 (405)	70.7 (487)	16.8

<sup>1</sup>Measured using elongation between the coupon shoulders after fracture

<sup>2</sup>The 0.2% offset method was used

### 3. Experimental Results

Local buckling typically led to the post-peak failure mechanisms, but local-distortional buckling interaction was observed, particularly in the 600S137-54 series specimens prior to peak load. As shown in Table 4, only a small variation in strength and stiffness is observed across all specimens of the same section type. Figure 6 contains the force-axial displacement plots for all columns tested and illustrates the consistency in strength across specimens with varying (even) fastener spacing and different EFG lengths. The even fastener spacing did not increase the local buckling capacity, but rather affected the location of local half-wavelengths. When possible, these local half-waves tended to occur between the fastener pairs on the web, as shown in Figure 7, and non-compatible buckling modes (webs buckling away from each other) were common. Increasing the EFG length, particularly in trials A1a through E1 with the 600S162-54 section, did not result in higher strengths. Previous work of the authors (Fratamico et al. 2016) on the global buckling and strength of 6 ft (1.83 m) long built-up CFS columns suggests a greater impact of the EFG on composite action; however, when local or distortional buckling are the dominant failure mode as in the tests presented here the EFG has considerably less of an effect on strength. For example, comparing results from trials A2 (no EFG) and D2 (13.5 in. (343 mm) EFG), a 53% increase in stiffness yet only a 4.0% increase in strength is achieved.

**Table 4. Test results with buckling and collapse behavior**

Trial ID	Even Spacing, $a$ [in.] (cm) <sup>1</sup>	EFG Length, $\alpha$ [in.] (cm)	Stiffness, $k$ [kip/in] (kN/mm) <sup>2</sup>	Elastic Buckling Mode	Compatible Web Buckling	Tested Strength, $P_u$ [kips] (kN)
A1a	36 (91)	0.0	353 (61.8)	L	No	31.7 (141)
A1b	36 (91)	0.0	379 (66.4)	L	No	31.4 (140)
A1c	36 (91)	0.0	386 (67.5)	L	No	31.4 (140)
A2	18 (46)	0.0	305 (53.4)	L-D	No	32.4 (144)
A3	12 (30)	0.0	309 (54.0)	L-D	Yes	31.4 (140)
A4	9 (23)	0.0	309 (54.0)	L-D	Yes	32.7 (145)
A5	6 (15)	0.0	399 (69.9)	L	Yes	34.4 (153)
B1	36 (91)	4.5 (11)	319 (55.9)	L-D	No	30.9 (138)
B2	18 (46)	4.5 (11)	436 (76.3)	L-D	Yes	32.6 (145)
B3	12 (30)	4.5 (11)	382 (66.9)	L-D	Yes	31.9 (142)
B4	9 (23)	4.5 (11)	426 (74.6)	L-D	Yes	31.7 (141)
B5	6 (15)	4.5 (11)	433 (75.8)	L-D	Yes	32.7 (146)
C1	36 (91)	9.0 (23)	366 (64.1)	L-D	Yes	32.3 (144)
C2	18 (46)	9.0 (23)	440 (77.0)	L-D	Yes	32.7 (145)
C3	12 (30)	9.0 (23)	415 (72.6)	L-D	Yes	31.8 (141)
C4	9 (23)	9.0 (23)	437 (76.5)	L-D	Yes	34.0 (151)
C5	6 (15)	9.0 (23)	407 (71.3)	L-D	Yes	33.2 (147)
D1	36 (91)	13.5 (34)	444 (77.7)	L-D	Yes	34.2 (152)
D2	18 (46)	13.5 (34)	468 (82.0)	L-D	Yes	33.7 (150)
E1	<i>full length</i>	<i>full length</i>	459 (80.3)	L-D	Yes	34.1 (151)
F1	36 (91)	0.0	473 (82.8)	L-D	No	27.7 (123)
F2	18 (46)	0.0	431 (75.6)	L-D	No	28.0 (125)
F3	12 (30)	0.0	344 (60.3)	L-D	Yes	27.2 (121)
F4	9 (23)	0.0	344 (60.3)	L-D	Yes	28.1 (125)
F5	6 (15)	0.0	347 (60.7)	L-D	Yes	28.0 (125)
G1	36 (91)	9.0 (23)	369 (64.6)	L-D	No	27.5 (122)
G2	18 (46)	9.0 (23)	341 (59.7)	L-D	Yes	28.4 (126)
G3	12 (30)	9.0 (23)	459 (80.3)	L-D	No	27.9 (124)
G5	6 (15)	9.0 (23)	376 (65.9)	L-D	Yes	28.5 (127)
H1	<i>full length</i>	<i>full length</i>	405 (70.9)	L-D	Yes	30.1 (134)

<sup>1</sup>For 36 in. (91 cm) spacing, true distance is smaller by twice the distance of the screw to the edge of the column, which is 0.375 in. (9.5 mm)

<sup>2</sup>Initial linear stiffness after full engagement of stud ends to tracks

A key effect both sought and observed in the tests was the level of compatible buckling, or degree of buckling conformity of both connected webs (and to some degree their connected flanges) in the built-up section. Buckling compatibility was visually observed and is recorded in Table 4. Compatible deformation modes continued from buckling to collapse in all cases. A decrease in the fastener spacing was shown to influence the level of compatible buckling, this is most evident in

the A-series results. At a spacing of  $L/3$  or less, compatible buckling is triggered, although an increase in stiffness or strength in trials A3, A4, and A5 is not achieved. Compatible buckling appears to be more influenced by the fastener spacing than the EFG length; however, when EFG lengths were long (series C, D, and G), the webs were more confined to move together. However, in longer columns, this effect of the EFG on compatible deformations may not be observed.

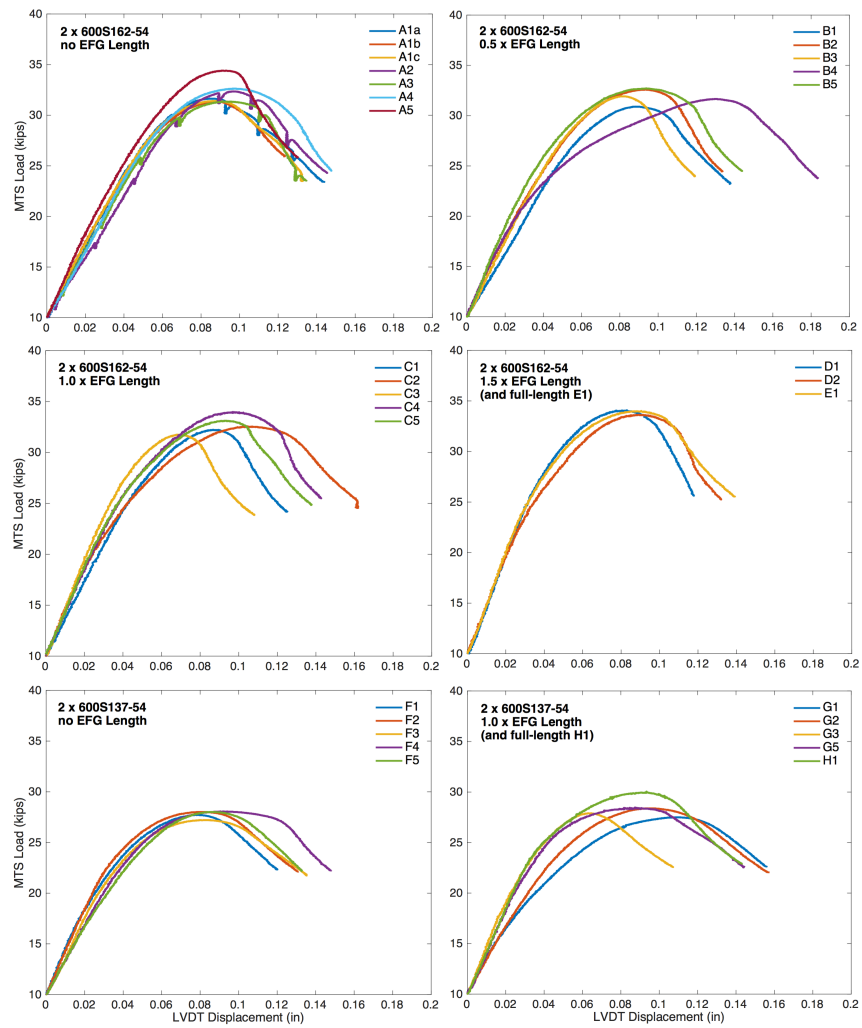


**Figure 6.** Load vs. axial displacement data across fastener spacings, but by section type & EFG length, removed early stud-to-track seating stiffness and displacements under 10 kips (44.5kN)

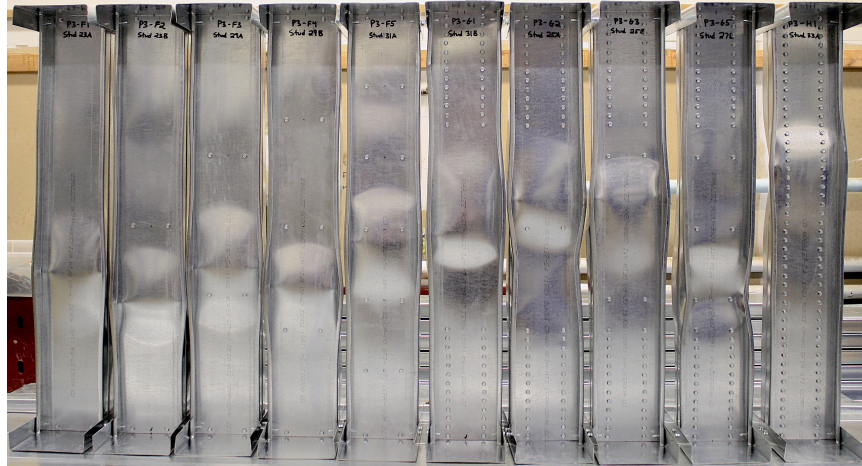


Figure 7. Frontal view of an example set of tested columns (of section type: 600S137-54)

The columns with the greatest capacity were the specimens with an extreme, full-length distribution of fasteners: trials E1 and H1. Compared with their  $L/1$  and no EFG cross-section equivalents, E1 and H1 had an increase in strength of 8.6% and 8.7%, respectively; however, there was no consistent increase in stiffness. Specimens E1 and H1 appeared to buckle in a local mode, but then demonstrate a more distortional deformation in the collapse regime, having a half-wavelength approximately one-third of the column height, as can be observed in the right-most specimen in Figure 7. To view a video of this column's behavior, as well as videos of other tests, please visit <http://tinyurl.com/hhg3fn2> for a full playlist.

Using position transducer (PT) data, local and distortional deformations were recorded for specimens that exhibited cross-section distortion at mid-height. Figure 8 shows the calculated metrics specific to back-to-back sections, assuming web buckling compatibility was achieved. Figure 9 shows the treatment of raw PT data for specimen G1, as an example, and displacements are taken from the PT data at peak load. The PT names, locations, and orientations are identical to those illustrated in Figure 4.

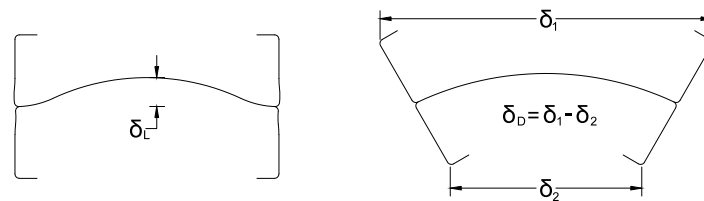
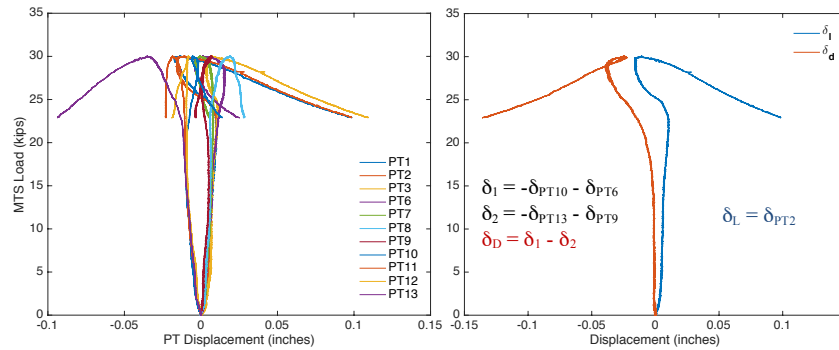


Figure 8. Local (left) and distortional (right) deformations of built-up CFS cross-sections



**Figure 9. Raw PT data from trial G1 (left) and calculated local and distortional cross-sectional deformations at peak load using specific PT data (right)**

**Table 5. Measured local and distortional deformations at peak load**

Trial ID	Deformation at Peak Load	Compatible Web Buckling	$\delta_L$ [in] (mm)	$\delta_D$ [in] (mm)
D2	Local-Distortional	Yes	0.206 (5.23)	0.640 (16.3)
G1	Local (Web)	No	0.201 (5.11)	0.118 (3.00)

Local and distortional deformations were calculated with the simple expressions shown in Figure 9, as negligible major or minor axis translation, or torsional rotation of the cross-section at mid-height was recorded or observed for the two given trials. In Table 5, specimens D2 and G1 are shown to exhibit a more local-distortional interaction buckling and local buckling-dominated failure, respectively. Local buckling is usually followed by a slight rotation of the flanges in the post-peak regime (a non-zero  $\delta_D$  in row 2 of Table 5) and distortional buckling mode 1 is always accompanied by out-of-plane web deformation (a non-zero  $\delta_L$  in row 1). The second plot of Figure 9 shows an inversion of the local buckling direction at peak load, as a plastic hinge develops. For all columns, the local failure mechanism observed was of the flip-disk type (Murray 1984). In some columns, well into the post-peak regime, a roof mechanism began to form, as can be seen in some of the 600S137-54 specimens in Figure 7.

#### 4. Discussion

In this experimental study, the variation of even screw spacing and EFG lengths were shown to have a small effect on column strength (a minor exception being the impractical detail of tightly spaced fasteners for the full-length, which did increase capacity). All of the conducted testing uses flat and level end bearing conditions and the stud is further attached to a track. The tests indicate that the end bearing condition may be more important than the EFG and even to a great

extent the fastener spacing. In the tests, an almost idealized fixed end condition is achieved via the seating of stud ends to the track, connection of stud flanges and track lips with screws, and the presence of EFG. These design components contribute to the end condition but are also competing to increase stiffness and strength in the columns, and they should be studied further in future work, particularly as a function of end bearing and for other end conditions on compression members such as in CFS truss chords.

Preliminary DSM strength predictions using nominal dimensions, but measured yield stress have been completed. If the elastic buckling assumes ideal fully-fixed ends and the fastener stiffness is approximated as smeared along the length, the results show the same trends as the tests, but are about 10% non-conservative. Evaluation using actual dimensions and considering different assumptions for the end conditions and fastener modeling are still in progress.

Local buckling drove post-peak behavior and failure in all of the columns except full-length fastener specimens E1 and H1. Although the local half-wavelengths changed location based on the screw spacings, the fastener layouts did not increase the local buckling capacities and column strengths even when compatible buckling in the web occurred. Two observations can be made from this: (1) local buckling is nearly unavoidable and design should not assume attached fasteners provide significant benefits against this mode, and (2) a dense array of web screws is not always required, and further work should address limits to screw spacings (and whether or not EFG are required) based on built-up column cross-section shapes and end conditions. When fewer screws are used, the columns are far easier to assemble and less expensive as well.

Comparing the two section types studied herein, the 600S162-54 and the 600S137-54 sections, the latter has a slightly higher distortional slenderness for both pinned and clamped end conditions due to its shorter flange width. Although local-distortional buckling controlled in trials F1-H1 with the 600S137-54 section, distortional post-peak behavior was observed in the trials with a denser layout of web screws and more compatible deformations of the web (namely, G5 and H1). Nevertheless, studies on built-up columns that have a distortional slenderness higher than their local and global slenderness should be performed to more closely correlate fastener layouts to distortional buckling behavior.

More experimental work is required to fully characterize built-up CFS column behavior. Tests on back-to-back CFS columns with web perforations and back-to-back and box section header beams completed in 2005 and 2003, respectively, at the Missouri University of Science and Technology catalyzed practical experimental research on simple CFS assemblies that is continued in the work

herein (LaBoube 2016). The goal is to continue to study as-constructed CFS assemblies, namely built-up columns, with both an experimental and numerical approach to address inadequacies in current design provisions and suggest more robust design approaches which account for all possible failure modes.

## **5. Conclusions**

Understanding the behavior and strength of screw-fastened built-up cold-formed steel (CFS) columns is important, as they are used frequently in frames as higher capacity columns, shear wall chord studs, among other applications. The tests herein show that the stiffness and strength of two studied built-up CFS columns, with stiff end bearing conditions, that buckle and fail in either local and/or distortional modes are not highly dependent on the layout of fasteners that connect the two members. In particular, a costly end fastener grouping consisting of a large series of fasteners at the member ends is not shown to appreciably improve the local and distortional buckling behavior or capacity of the built-up CFS column. Ongoing work will aim to develop better design methods that incorporate more accurate estimations of column end conditions and require the explicit modeling of web fasteners. Additional work is needed to provide experimental data on different built-up cross-section types, fastener details and layouts, and primary limit states. Subsequent tests are underway to continue to explore primary deformation modes of built-up columns.

## **Acknowledgements**

Research for this paper was conducted with partial U.S. Government support under FA9550-11-C-0028 and awarded by the Department of Defense, Air Force Office of Scientific Research, National Defense Science and Engineering Graduate (NDSEG) Fellowship, 32 CFR 168a. The senior authors would also like to acknowledge support from the Australian Research Council for collaboration on this topic under Discovery Project DP140104464. Special thanks to Nick Logvinovsky for his assistance in lab apparatus assembly and to fellow Ph.D. candidate Xi Zhao for her ongoing cooperation with the first author on an ongoing project on quantification of imperfections in built-up CFS members. Lastly, thanks to ClarkDietrich Building Systems and Simpson Strong-Tie for graciously providing all CFS sections and screw fasteners, respectively. Any opinions, findings, and conclusions or recommendations expressed in this material are those of the author(s) and do not necessarily reflect the views of sponsors or other participants.

## References

- AISC 360 (2010). *Specification for Structural Steel Buildings*, American Institute of Steel Construction, Chicago, IL.
- AISI-S100 (2012). *North American Specification for the Design of Cold-Formed Steel Structural Members*, American Iron and Steel Institute, Washington, D.C.
- American Society for Testing and Materials (ASTM), Standard Test Methods and Definitions for Mechanical Testing of Steel Products (ASTM370-12a), ASTM, West Conshohocken, PA, 2012.
- Anbarasu, M., Kanagarasu, K., Sukumar, S. (2015). "Investigation on the behaviour and strength of cold-formed steel web stiffened built-up batten columns." *Materials & Structures*, 48, 4029-4038.
- Dabaon, M., Eloobody, E., Ramzy, K. (2015). "Experimental investigation of built-up cold-formed steel section batten columns." *Thin-Walled Structures*, 92, 137-145.
- Fratamico, D.C. and Schafer, B.W. (2014). "Numerical Studies on the Composite Action and Buckling Behavior of Built-Up Cold-Formed Steel Columns." 22<sup>nd</sup> Int'l. Spec. Conf. on Cold-Formed Steel Structures, St. Louis, MO.
- Fratamico, D.C., Torabian, S., Schafer, B.W. (2015). "Composite Action in Global Buckling of Built-Up Columns Using Semi-Analytical Fastener Elements." Proc. of the Annual Stability Conf., Structural Stability Res. Co., Nashville, TN.
- Fratamico, D.C., Torabian, S., Rasmussen, K.J.R., Schafer, B.W. (2016). "Experimental Studies on the Composite Action in Wood-Sheathed and Screw-Fastened Built-Up Cold-Formed Steel Columns." Proc. of the Annual Stability Conf., Structural Stability Res. Co., Orlando, FL.
- Georgieva, I., Schueremans, L., Pyl, L. (2012). "Composed columns from cold-formed steel Z-profiles: Experiments and code-based predictions of the overall compression capacity." *Engineering Structures*, 37, 125-134.
- Georgieva, I., Schueremans, L., Pyl, L., Vandewalle, L. (2012). "Experimental investigation of built-up double-Z members in bending and compression." *Thin-Walled Structures*, 53, 48-57.
- Georgieva, I., Schueremans, L., Vandewalle, L., Pyl, L. (2012). "Design of built-up cold-formed steel columns according to the direct strength method." *Procedia Engineering*, 40, 119-124.
- LaBoube, R. (2016). "Cold-Formed Steel – Res. to Practice." Proc. of the Annual Stability Conf., Structural Stability Res. Co., Orlando, FL.
- Lama Salomon, A., Fratamico, D.C., Schafer, B.W., Moen, C.D. (2016). "Full field cold-formed steel column buckling measurements with high resolution image-based reconstruction." Proc. of the Annual Stability Conf., Structural Stability Res. Co., Orlando, FL.
- Murray, Noel W. Introduction to the Theory of Thin-walled Structures. Oxford: Clarendon Press, 1984.
- Schafer, B.W. and Ádány, S. (2006). "Buckling analysis of cold-formed steel members using CUFSM: conventional and constrained finite strip methods." 18<sup>th</sup> Int'l. Spec. Conf. on Cold-Formed Steel Structures, Orlando, FL.
- Stone, T.A. and LaBoube, R.A. (2005). "Behavior of cold-formed steel built-up I-sections." *Thin-Walled Structures*, 43(12), 1805-1817.
- Torabian, S., Zheng, B., and Schafer, B.W. (2015). "Experimental response of cold-formed steel lipped channel beam-columns." *Thin-Walled Structures*, 89, 152-168.
- Wang, L. *Structural behaviour of cold-formed steel built-up section beams*. Ph.D. Thesis, The University of Hong Kong; 2015.
- Young, B. and Chen, J. (2008). "Design of Cold-Formed Steel Built-Up Closed Sections with Intermediate Stiffeners." *Journal of Structural Engineering*, ASCE, 134, 727-737.
- Zhang, J. *Cold-formed steel built-up compression members with longitudinal stiffeners*. Ph.D. Thesis, The University of Hong Kong; 2014.
- Zhao, X., Tootkaboni, M., Schafer, B.W. (2015). "Development of a Laser-Based Geometric Imperfection Measurement Platform with Application to Cold-Formed Steel Construction." *Experimental Mechanics*, 55, 1779-1790.
- Zhao, X. and Schafer, B.W. (2016). "Measured geometric imperfections for Cee, Zee, and Built-up cold-formed steel members." 23<sup>rd</sup> Int'l. Spec. Conf. on Cold-Formed Steel Struc., Baltimore, MD.